A Study into the Stability of 3,6-Dihydro-2*H*-thiopyran Rings: Key Linkages in the RAFT Hetero-Diels−Alder *Click* Concept

Sebastian Sinnwell,[†,‡] **Christopher V. Synatschke,**[‡] **Thomas Junkers,**[†]
Martina H. Stenzel,*[‡] **and Christopher Barner-Kowollik***[†]

Preparative Macromolecular Chemistry, Institut für Technische Chemie and Polymer Chemie, Universität Karlsruhe (TH)/Karlsruhe Institute of Technology (KIT), Engesserstr. 18, 76128 Karlsruhe, Germany, and Centre for Advanced Macromolecular Design (CAMD), School of Chemical Sciences and Engineering, The University of New South Wales, Sydney NSW 2052, Australia

Received June 21, 2008; Revised Manuscript Received September 5, 2008

ABSTRACT: The combination of RAFT chemistry and hetero-Diels−Alder (HDA) cycloaddition provides a convenient conjugation tool for the construction of macromolecular architectures. The actual conjugation linkage, which is formed in the RAFT HDA approach, consists of a 3,6-dihydro-2*H*-thiopyran ring. Herein, a careful study into the stability of polymer linked by 3,6-dihydro-2*H*-thiopyran rings under different thermal and pH conditions is performed. As polymeric model system, a 3,6-dihydro-2*H*-thiopyran functionalized poly(ethylene glycol) (PEG) obtained after a HDA cycloaddition between a diene functionalized PEG and 1-phenylethyl (diethoxyphosphoryl)dithioformate or 1-phenylethyl pyridin-2-yldithioformate is used. Electrospray ionization mass spectrometry (ESI-MS) is employed to map the generated products. The stability tests under thermal conditions showed for the diethoxyphosphoryl derivative the preservation of the polymer end-groups after 24 h at temperatures up to 80 °C. At higher temperatures degradation reactions of the 3,6-dihydro-2*H*-thiopyran ring including the retro HDA reaction occurred. A complete fragmentation was observed after 24 h at 160 °C. The pyridinyl derivative was found to be slightly more temperature stable since its structure was unaffected at conditions up to 24 h at 120 °C and full cleavage was only observed after 24 h at 180 °C. In this case the fragmentation mechanism occurred exclusively via the retro HDA reaction and the resulting diene functionalized polymer was the only detected product species. Both conjugates showed an excellent stability toward hydrolysis in aqueous media under strong acidic (0.1 and 1 M HCL) and strong basic (0.1 and 1 M NaOH) conditions.

Introduction

Over the past decade, the development of living/controlled radical polymerization (CRP) techniques has allowed for the synthesis of a variety of macromolecular architectures of well-defined structure and functionality.[1] Especially the polymerization via reversible addition-fragmentation transfer (RAFT) is a versatile method applicable for most monomers and under a wide range of conditions.[2] The nearly quantitative incorporation of the Z and R groups of the RAFT agents as polymer end-groups offers a convenient access to end-group functionalized polymers.[3] Functionalities like carboxyl, hydroxyl and others have been introduced via this approach and were used for further post-polymerization end-group modifications. The intrinsic end-group functionality of all RAFT polymers, however, is the thiocarbonylthio group whose retention is responsible for the living/controlled character of the polymerization. In addition to its function as chain transfer agents (CTA), the thiocarbonylthio groups of RAFT polymers can also be used as precursors for post-polymerization transformations. In this context the options vary from thermolysis,[4−6] hydrolysis,[7,8] or aminolysis[9] to reduction[10] or oxidation.[11]

Recently, our laboratories described the conversion of electron deficient dithioester end-groups of RAFT polymers via hetero-Diels−Alder (HDA) cycloadditions with suitable dienes as a facile end-group transformation. In this atom-economical approach, polymer conjugates such as block copolymers,[12] star-shaped polymers,[13] star-shaped block copolymers[14] and surface modified microspheres[15] were successfully generated. The utilized RAFT agents have been carefully chosen since the general ability of dithioesters to undergo HDA cycloadditions, which leads to the formation of 3,6-dihydro-2*H*-thiopyran heterocycles (Scheme 1), is rather low.[16] Their efficiency as heterodienophiles, however, can be remarkably improved by attaching electronwithdrawing substituents in α-position (CN,[17] COOR,[18] CF_3,[19] SO_2R,[20] $PO(OR)_2$,[21,22] pyridinyl)[23] which lower the LUMO energy of the thiocarbonyl group. For the actual RAFT HDA approach, benzyl (diethoxyphosphoryl)dithioformate and benzyl pyridin-2-yldithioformate have been used as CTAs so far and were found to provide an adequate polymerization control as well as a high efficiency for the post-polymerization conjugation reaction. The stability of the actual linkage, which consists of a 3,6-dihydro-2*H*-thiopyran ring, was only briefly investigated. Whereas the structure of block copolymers remained unaffected after 24 h at 60 °C,[12] experiments with poly(styrene) 4-arm star polymers indicated a complete cleavage of the poly(styrene) arms from the core after being subjected to 160 °C for 24 h.[13] Thus, in contrast to alkyne−azide click routes which find repeated application in the contemporary literature,[24] the RAFT HDA approach provides an atom-efficient orthogonal conjugation method in which the polymer segments are cleaved in response to an external (thermal) stimulus. This behavior is of potential interest because it provides the possibility for the generation of polymer architectures with predetermined fragmentation patterns while at the same time being of high stability at ambient conditions. The applications of these materials may include fields like molecular imprinting, smart materials, and biomedical disciplines.

In order to investigate the possibilities of induced cleavage of the RAFT HDA approach, the present contribution features

---

* Corresponding authors. (C.B-K.) Fax: +49 721 6085740. E-mail: christopher.barner-kowollik@polymer.uni-karlsruhe.de. (M.H.S.) Fax: +61 2 93856250. E-mail: m.stenzel@unsw.edu.au.

[†] Preparative Macromolecular Chemistry, Institut für Technische Chemie and Polymer Chemie, Universität Karlsruhe (TH)/Karlsruhe Institute of Technology (KIT).

[‡] Centre for Advanced Macromolecular Design (CAMD), School of Chemical Sciences and Engineering, The University of New South Wales.

10.1021/ma8013959 CCC: $40.75

Scheme 1. Hetero-Diels−Alder Cycloaddition of Electron-Deficient Dithioesters

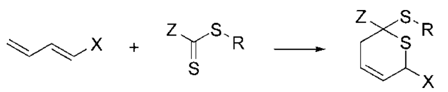

Scheme 2. 3,6-Dihydro-2*H*-thiopyran Functionalized Poly(Ethylene glycol) 6 and 7

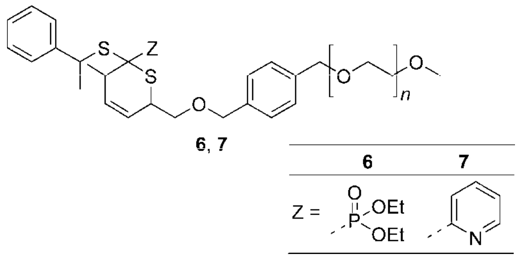

a careful study into the stability of polymer linked 3,6-dihydro-2*H*-thiopyran rings under different thermal and pH conditions. As polymeric model system, a 3,6-dihydro-2*H*-thiopyran functionalized poly(ethylene glycol) (PEG) obtained after a HDA cycloaddition between a diene functionalized PEG and 1-phenylethyl (diethoxyphosphoryl)dithioformate or 1-phenylethyl pyridin-2-yldithioformate is used (Scheme 2). A PEG system was chosen due to its excellent ionizablility in ESI-MS measurements and its high thermal and hydrolytic stability. Electrospray ionization mass spectrometry (ESI-MS) is employed to map the generated products. The ESI-MS methodology facilitates the mapping of structural details of individual polymer chains with a high degree of accuracy and sensitivity. Due to the particularly soft ionization technique it is especially suitable to study polymer end-group compositions and degradation[25,26] which allows for insights into polymerization mechanisms.[27]

Experimental Section

Materials and Methods. 2-Benzenesulfonylmethylpyridine was synthesized according to the literature.[28] *trans*,*trans*-2,4-Hexadien-1-ol (97%, Aldrich), 1,4-bis(bromomethyl)benzene (97%, Aldrich), sodium hydride (60% dispersion in mineral oil, Aldrich), poly(ethylene glycol) monomethylether 1100 (Fluka), tetrahydrofurane (THF, anhydrous, ≥ 99.9%, Sigma-Aldrich), diethyl phosphite (>99.0%, Fluka), carbon disulfide (analytical reagent, Ajax Finechem), (1-bromoethyl)benzene (97%, Aldrich), elemental sulfur (APS), trifluoroacetic acid (TFA, 99%, Sigma-Aldrich), and potassium *tert*-butoxide (>97%, Fluka) were used as received.

^{1}H and ^{13}C NMR spectra were measured on a Bruker DPX 300 spectrometer at 300 MHz for hydrogen and 75 MHz for carbon nuclei. All samples were dissolved in chloroform-d. ESI-MS measurements were performed on a Thermo Finnigan LCQ Deca quadrupole ion trap mass spectrometer (Thermo Finnigan, San Jose, CA) equipped with an atmospheric pressure ionization source operating in the nebulizer assisted electrospray mode which was used in positive ion mode. Polymer samples (0.1−0.2 mg·mL^{-1}) were dissolved in 3:2 v/v mixture of THF and methanol (MeOH) doped with sodium acetate (0.05−0.1 mg·mL^{-1}). Mass calibration was performed using caffeine, Met-Arg-Phe-Ala acetate salt (MRFA, Sigma-Aldrich) and Ultramark 1621 (Sigma-Aldrich) in the m/z range 195−1822. All spectra were acquired within the m/z range of 150−2000 with a spray voltage of 5 kV and a capillary temperature of 275 °C. Nitrogen was used as a sheath gas (flow: 45% of maximum) and helium was used as the auxiliary gas (flow: 5% of maximum). The error over the m/z axis of the used setup comes to $\Delta m/z = 0.1 - 0.2$. Depending on the calibration of the instrument, larger absolute deviations from the theoretical m/z were sometimes observed with the PEG samples. However, in those cases, a general shift of all peaks is observed so that a maximum uncertainty of about $\Delta m/z = 0.1$ remains when the spectrum is referenced to a known repeating species. To allow for such "internal calibration", the identity of peaks was confirmed by high-resolution Q-TOF measurements using a setup as described earlier.[26] Theoretical masses were calculated by using the IsotopeViewer Version 1.0 software.

Synthesis of 1-((*trans*,*trans*-Hexa-2,4-dienyloxy)methyl)-4-(bromomethyl)benzene (1). 1,4-Bis(bromomethyl)benzene (9.39 g, 35.6 mmol) and sodium hydride (843 mg, 21.1 mmol) were placed in a 250 mL round-bottom flask equipped with a magnetic stirrer. After the addition of 80 mL THF, the flask was sealed with a rubber septum, purged with nitrogen and *trans*,*trans*-2,4-hexadien-1-ol (1.74 g, 17.8 mmol) in 3 mL of THF was given dropwise to the solution at room temperature. After the complete addition, the mixture was stirred for further 6 h at room temperature. The mixture was washed with 20 mL of aqueous ammonium chloride solution (1 M) in order to destroy the residual sodium hydride. After the removal of the solvent and addition of 80 mL *n*-hexane, the mixture was stored at −19 °C overnight. The solidified unreacted 1,4-bis(bromomethyl)benzene starting material was removed via filtration and then washed with hexane. The filtrate was reduced in vacuum to a volume of 20 mL and directly chromatographed over silica gel. After drying over magnesium sulfate and evaporation of the solvent, the product was obtained as a clear liquid. Yield: 29%. R_f: 0.20 (SiO_2, *n*-hexane/ethyl acetate, 99:1). ^{1}H NMR (300 MHz, $CDCl_3$, δ, ppm): 1.76 (d, $J = 6.8$ Hz, 3H), 4.04 (d, $J = 6.4$ Hz, 2H), 4.50 (s, 4H), 5.6−5.8 (m, 2H), 6.0−6.3 (m, 2H), 7.3−7.4 (m, 4H). ^{13}C NMR (75 MHz, $CDCl_3$, δ, ppm): 18.0 ($-\mathbf{C}H_3$), 33.3 ($-\mathbf{C}H_2Br$), 70.6 ($ArCH_2O\mathbf{C}H_2-$), 71.3 ($Ar\mathbf{C}H_2OCH_2-$), 126.4, 130.1, 130.7, 133.4 (4 dieneC), 128.0, 129.0, 137.0, 138.8 (6 ArC).

Synthesis of Diene-Functionalized Poly(ethylene glycol) (3). Under a nitrogen atmosphere, 1-((*trans*,*trans*-hexa-2,4-dienyloxy)methyl)-4-(bromomethyl)benzene **1** (1.50 g, 5.34 mmol) in 2 mL of THF was added to a suspension of sodium hydride (488 mg, 12.2 mmol) in 60 mL of THF. After the addition of poly(ethylene glycol) **2** (3.13 g, 2.66 mmol) under a nitrogen counter flow, the mixture was stirred overnight at room temperature. The mixture was washed with 20 mL aqueous ammonium chloride solution (1 M) and the aqueous phase extracted twice with chloroform. Polymer **3** was isolated by precipitation into cold diethylether, filtration and drying under reduced pressure. Yield: 85% ^{1}H NMR (300 MHz, $CDCl_3$, δ, ppm): 1.74 (d, $J = 6.8$ Hz, 3H), 3.37 (s, 3H), 3.63 (s, $(-OCH_2CH_2)_n-$), 4.01 (d, $J = 6.3$ Hz, 2H), 4.48 (s, 2H), 4.54 (s, 2H), 5.6−5.8 (m, 2H), 6.0−6.3 (m, 2H), 7.30 (s, 4H). ^{13}C NMR (75 MHz, $CDCl_3$, δ, ppm): 18.0 ($-CH\mathbf{C}H_3$), 58.9 ($-O\mathbf{C}H_3$), 69.3 ($ArCH_2O\mathbf{C}H_2CH_2-$), 70.5 ($-(O\mathbf{C}H_2\mathbf{C}H_2)_n-$), 71.5 ($ArCH_2O\mathbf{C}H_2CH-$), 71.8, ($Ar\mathbf{C}H_2O-$), 72.9 ($Ar\mathbf{C}H_2O-$), 127.7 (4 ArC), 126.5, 129.9, 130.7, 133.2 (4 dieneC), 137.5, 137.7 (2 ArC).

Synthesis of 1-Phenylethyl (Diethoxyphosphoryl)Dithioformate (4). RAFT agent **4** was synthesized based on a procedure published in the literature.[29] Under a nitrogen atmosphere, diethyl phosphite (2.05 mL, 2.20 g, 15.9 mmol) in 7 mL THF was added dropwise to a suspension of NaH (647 mg, 16.2 mmol) in 15 mL of THF. After the evolution of hydrogen was finished, the reaction mixture was stirred for 15 min. The mixture was then cooled in an ethanol/dry ice bath and carbon disulfide (4.6 mL, 5.81 g, 76.3 mmol) was added under stirring. The mixture was allowed to warm to room temperature and was stirred for further 30 min. (1-bromoethyl)benzene (2.45 mL, 3.32 g, 17.95 mmol) was added followed by 18 h stirring at room temperature. After *n*-hexane (30 mL) was given to the mixture, it was filtered and the solvent removed from the filtrate under reduced pressure. The product was chromatographed over silica gel, first with cyclohexane to remove impurities and then with diethylether to collect the product. After removal of the solvent the dithioformate **4** could be obtained as a pink liquid. Yield: 29%. ^{1}H NMR (300 MHz, $CDCl_3$, δ, ppm): 1.30 (t, $J = 7.0$ Hz, 3H), 1.32 (t, $J = 7.0$ Hz, 3H), 1.69 (d, $J = 7.1$ Hz, 3H), 4.1−4.3 (m, 4H), 5.17 (q, $J = 7.1$ Hz, 3H) 7.2−7.4 (m, 5H). ^{13}C NMR (75 MHz, $CDCl_3$, δ, ppm): 16.2 (d, $J = 5.1$ Hz, 2

$-\mathrm{OCH_2}\mathbf{C}\mathrm{H_3}$), 20.0 ($-\mathrm{CH(}\mathbf{C}\mathrm{H_3)}-$), 48.4 (d, J = 2.9 Hz, ($-\mathbf{C}\mathrm{H(CH_3)}-$), 64.5 (d, J = 6.5 Hz, ($-\mathbf{O}\mathrm{CH_2CH_3}$)^a), 64.6 (d, J = 6.5 Hz, ($-\mathbf{O}\mathrm{CH_2CH_3}$)^b) 127.7, 127.9, 128.6, 139.9 (6 ArC), 227.1 (d, J = 174 Hz, $-\mathrm{S(}\mathbf{CS}\mathrm{)}-$).

Synthesis of 1-Phenylethyl Pyridin-2-yldithioformate (5). RAFT agent **5** was synthesized based on a procedure published in the literature.[30] Potassium *tert*-butoxide (20.38 g, 181.6 mmol) was added under stirring to a mixture of 2-benzenesulfonylmethylpyridine (14.41 g, 61.8 mmol) and elemental sulfur (5.80 g, 181 mmol) in THF (200 mL). During the addition, the color of the mixture changed to dark brown. After stirring the mixture at room temperature for 16 h, (1-bromoethyl)benzene (33.4 g, 180.5 mmol) was added dropwise. The color of the solution turned into a dark red and stirring was continued for 1 h. The organic solution was washed with deionized water and the aqueous phase extracted three times with dichloromethane. The combined organic phases were dried over magnesium sulfate, the solvent was evaporated and the product chromatographed over silica gel with dichloromethane as eluent. Upon removal of the solvent the dithioformate **5** could be isolated as a dark red liquid. Yield: 28%. ^{1}H NMR (300 MHz, $\mathrm{CDCl_3}$, δ, ppm): 1.85 (d, J = 7.2 Hz, 3H), 5.25 (q, J = 7.2 Hz, 1H), 7.24 − 7.40 (m, 3H), 7.45 (ddd, J_1 = 7.6 Hz, J_2 = 4.8 Hz, J_3 = 1.3 Hz, 1H), 7.47 − 7.52 (m, 2H) 7.76 (ddd, J_1 = 7.8 Hz, J_2 = 7.8 Hz, J_3 = 1.8 Hz, 1H), 8.31 (ddd, J_1 = 8.1 Hz, J_2 = 1.0 Hz, J_3 = 1.0 Hz, 1H), 8.61 (ddd, J_1 = 4.7 Hz, J_2 = 1.8 Hz, J_3 = 0.9 Hz, 1H). ^{13}C NMR (75 MHz, $\mathrm{CDCl_3}$, δ, ppm): 20.8 ($-\mathrm{CH(}\mathbf{C}\mathrm{H_3)}-$), 48.8 ($-\mathbf{C}\mathrm{H(CH_3)}-$), 122.3, 126.6, 127.4, 127.9, 128.5, 136.8, 141.5, 147.8, 156.5 (9 ArC), 224.7 ($-\mathrm{S(}\mathbf{CS}\mathrm{)}-$).

Hetero-Diels−Alder Cycloaddition between the Diene Functionalized PEG 3 and RAFT Agent 4 (6). Diene functionalized PEG **3** (500 mg, 0.385 mmol), dithioformate **4** (245 mg, 0.77 mmol), zinc chloride (1.1 equiv, 116 mg, 0.85 mmol) and chloroform (6 mL) were placed in a flask and sealed with a rubber septum. In order to dissolve the zinc chloride, the mixture was placed in an ultrasonic bath for a few minutes. The solution was kept at 50 °C under stirring for 24 h. The solvent was evaporated and the product stored at −19 °C.

Hetero-Diels−Alder Cycloaddition between the Diene Functionalized PEG 3 and RAFT Agent 5 (7). Diene functionalized PEG **3** (500 mg, 0.385 mmol), dithioformate **5** (200 mg, 0.77 mmol) and trifluoroacetic acid (1.1 equiv, 97 mg, 0.85 mmol) dissolved in chloroform (6 mL) were placed in a sealed flask and heated at 50 °C under stirring for 24 h. The solvent was evaporated and the product stored at −19 °C.

Thermal Stability of 6 and 7. In a typical experiment the hetero-Diels−Alder adduct (**6**, 16.1 mg, 10 μmol or **7**, 15.5 mg, 10 μmol) was dissolved in toluene (5 mL) and placed in a pressure resistant glass tube. The mixtures were heated to the according temperature in a thermostatted oil bath for 24 h. At the end of the reaction time the solvent was evaporated.

pH Stability of 6 and 7. In a typical experiment the hetero-Diels−Alder adduct (**6**, 12 mg, 7.5 μmol or **7**, 12 mg, 7.7 μmol) was dissolved in aqueous solutions (5 mL) of sodium hydroxide (1 M and 0.1 M) or hydrochloric acid (1 M and 0.1 M). After stirring the solutions for 24 h at room temperature the organic compounds were extracted with $\mathrm{CHCl_3}$, the organic phases combined and the solvent evaporated under reduced pressure.

Results and Discussion

Scheme 3. Synthesis of the Diene Functionalized PEG 3 via an Asymmetric Etherification of 1,4-Bis(Bromomethyl)Benzene

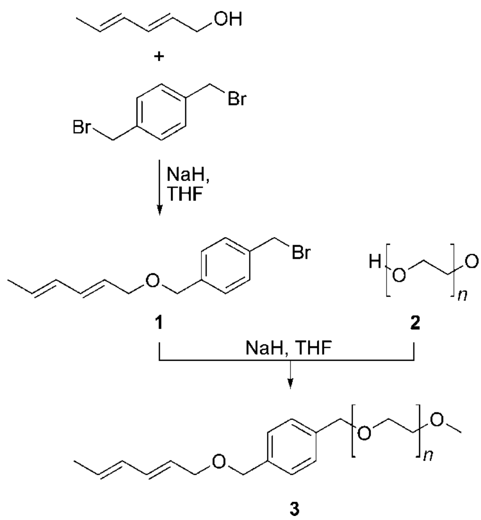

Synthesis of the Diene Functionalized PEG 3. The preparation of the diene functionalized PEG **3** was carried out via two consecutive etherification reactions as shown in Scheme 3. Due to the later following stability studies of the HDA modified PEG **6** and **7** (see Scheme 2), which are based on compound **3**, ether linkages were chosen for the construction of the diene functionalized PEG. Alternative linkages, for example, esters would not resist the strong basic or acidic condition of the later experiments. In the first step, 1,4-bis(bromomethyl)benzene was reacted with 2,4-hexadiene-1-ol in a nucleophilic substitution reaction. In order to suppress the substitution of both bromides on the same molecule, 1,4-bis(bromomethyl)benzene was used in excess compared to the alcohol. The successful synthesis of **1** was confirmed by NMR spectroscopic methods, which clearly show a characteristic asymmetric substituent pattern of **1** (see Experimental Section).

In the second step, compound **1** was reacted with PEG **2** under similar conditions as in the synthesis of **1**. In order to be able to analyze the polymer samples of later experiments via ESI-MS, which has in the used setup a detection limit of m/z = 2000, the PEG starting material **2** was chosen with a number-average molar mass, M_n, of 1100 g mol^{-1}. The ^{1}H NMR spectrum of the obtained PEG **3** shows the presence of both the polymer backbone and the vinylic protons (Figure SI-1, Supporting Information). A comparison of the signal intensities of the protons of both end-groups reveals the quantitative diene functionalization of **3**. To further confirm the structural uniformity of **3**, ESI-MS measurements were performed. In the full spectrum (Figure 1a), one series of signals with a maximum in intensity at m/z = 1268.1 dominates and can be assigned to the different chain lengths of the diene functionalized PEG **3** cationized with Na$^+$. Two additional series of signals of minor intensity are assigned to potassium molecule ions of **3** as well as to the sodium molecule ions of the starting material **2**. A zoom of the 1260−1305 m/z region which includes the signal with the highest intensity is shown in Figure 1b. The experimental m/z values of the three peaks in this zoom region are compared to the theoretical values of the corresponding ion assignments, as summarized in Table 1, confirming the structures of PEG **3** (as Na$^+$ and K$^+$ adducts) and residual starting material **2**. The measurement shows a slight general shift of m/z_{expt} as compared to the theoretical values which may be attributed to the peculiarity of the ESI-MS analysis of the PEG samples (see Experimental Section). Due to the high ionizablity of PEG, also multiple charged species appear as subdistributions in the spectrum. They are easily identified as double charged species by means of the distance between the peaks in their isotopic pattern of $\Delta m/z$ = 0.5 and by the seemingly reduced repetition unit of $\Delta m/z$ = 22 instead of 44. For all subsequent discussions only single-charged adducts are discussed as no additional information can be deduced from the multiple charged states.

HDA Cycloadditions between the Diene Functionalized PEG 3 and RAFT Agents 4 and 5. In order to convert the diene functionalized PEG **3** via a HDA cycloaddition, RAFT agents **4** and **5** were synthesized. These compounds, which carry a diethoxyphosphoryl and a pyridinyl Z group, respectively,

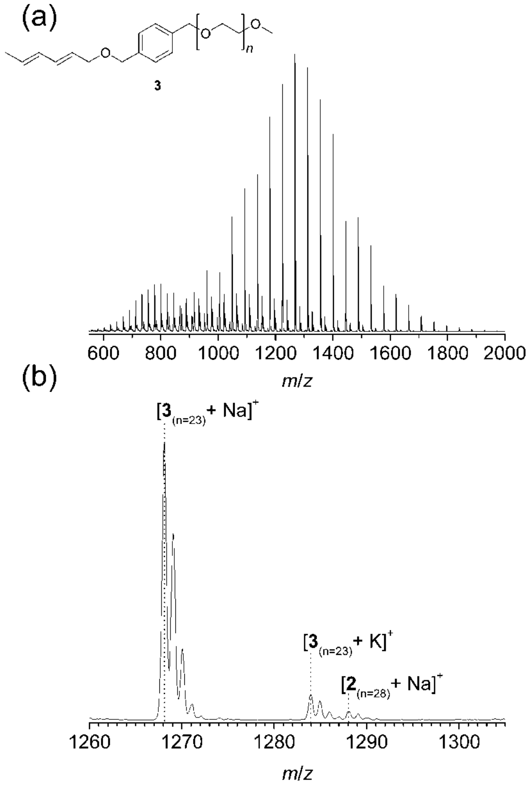

Figure 1. (a) Full ESI-MS spectrum and (b) 1260−1305 *m/z* region of the diene functionalized PEG **3** after etherification of PEG monomethylether **2** with 1-((*trans*,*trans*-hexa-2,4-dienyloxy)methyl)-4-(bromomethyl)benzene **1** (NaH, THF, 6 h, room temperature).

Table 1. Experimental and Theoretical *m/z* Values for the First Peak in the Isotopic Distributions of the Zoom Spectrum in Figure 1b and Their Assignment

m/z_{expt}	ion assignment	formula	m/z_{theor}	$\Delta m/z$
1268.1	PEG $3_{(n=23)}$ + Na^+	$[C_{61}H_{112}O_{25}Na]^+$	1267.7	0.4
1283.9	PEG $3_{(n=23)}$ + K^+	$[C_{61}H_{112}O_{25}K]^+$	1283.7	0.2
1288.1	PEG $2_{(n=28)}$ + Na^+	$[C_{57}H_{116}O_{29}Na]^+$	1287.8	0.3

represent the two types of electron deficient RAFT agents which have been utilized in the RAFT HDA approach so far. They are slightly modified in structure compared to those used in previous investigations[12−15] as they carry a 1-phenylethyl instead of a benzyl R group. This modification was chosen in order to provide a better model for polymeric RAFT systems in which the polymer end-groups usually consist of secondary or tertiary leaving groups. In fact, previous investigations concerning the thermal decomposition of RAFT agents during polymerizations have shown that the 1-phenylethyl R group provides an excellent mimic for the repeating unit of a poly(styrene) chain.[4]

The HDA cycloaddition between PEG **3** and RAFT agents **4**, **5** were performed under similar conditions as in the polymer conjugation approaches described in the literature (use of zinc chloride as the catalyst in case of **4** and trifluoroacetic acid in case of **5**, chloroform solution, 50 °C, 24 h).[12−15] Both obtained end-group modified polymers **6** and **7** carry the desired 3,6-dihydro-2*H*-thiopyran structure (Scheme 4) but differ in their substituent in 2-position which is diethoxyphosphoryl in case of **6** and pyridine-2-yl in case of **7**, the former Z groups of the RAFT agents **4** and **5**.

Due to the number of possible isomers of the 3,6-dihydro-2*H*-thiopyran ring which are formed in the HDA cycloaddition, the NMR data of the heterocyclic end-group in **6** and **7** are complex. Figure SI-2 (Supporting Information) shows the ^{1}H NMR spectrum of PEG **6**. It is clearly possible to observe the disappearance of the signals of two of the four vinylic protons (four multiplets between 5.6 and 6.3 ppm) as well as of the methylene group in the allyl position (doublet at 4.01 ppm) of the starting material **3** after the HDA reaction suggesting a successful conversion of **3**. Considering that the possible stereo isomers may differ in their spectroscopic properties but not in their mass, ESI-MS measurements were performed in order to demonstrate the successful end-group modification. Figure 2a shows the complete ESI-MS spectrum of the HDA reaction

Scheme 4. Hetero-Diels−Alder Cycloaddition between the Diene Functionalized PEG 3 and RAFT Agents 4 and 5 (use of Zinc Chloride as the Catalyst in Case of 4 or Trifluoroacetic Acid in Case of 5, Chloroform Solution, 50 °C, 24 h)

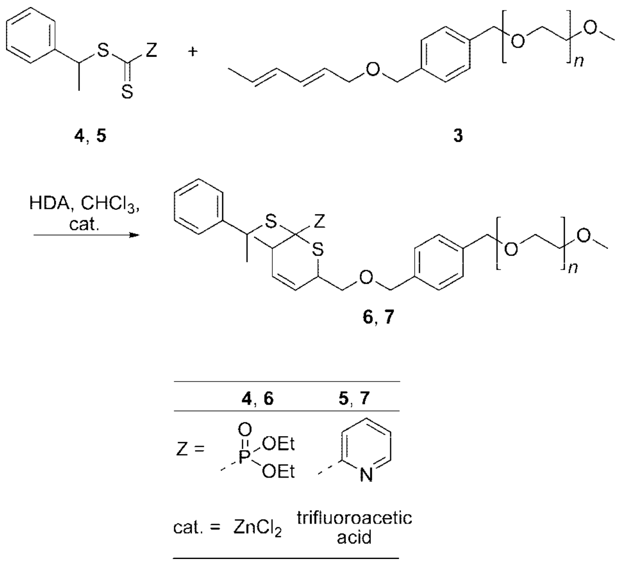

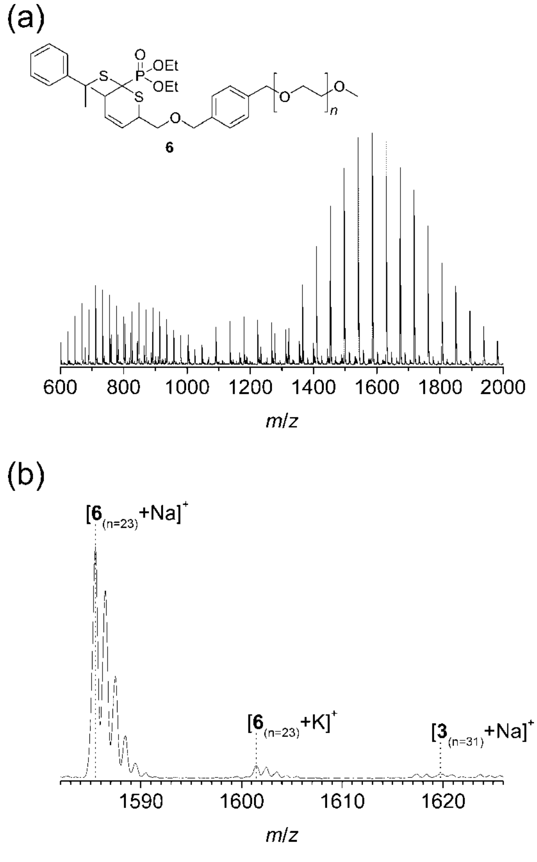

Figure 2. (a) Full ESI-MS spectrum and (b) 1582−1626 *m/z* region of PEG **6** after the HDA cycloaddition between RAFT agent **4** and PEG **3** (zinc chloride as the catalyst, chloroform, 24 h, 50 °C).

Table 2. Experimental and Theoretical *m/z* Values for the First Peak in the Isotopic Distributions of the Zoom Spectrum in Figure 2b and Their Assignment

m/z_{expt}	ion assignment	formula	m/z_{theor}	$\Delta m/z$
1585.5	PEG $6_{(n=23)}$ + Na$^+$	$[C_{74}H_{131}O_{28}PS_2Na]^+$	1585.8	0.3
1601.5	PEG $6_{(n=23)}$ + K$^+$	$[C_{74}H_{131}O_{28}PS_2K]^+$	1601.8	0.3
1619.9	PEG $3_{(n=31)}$ + Na$^+$	$[C_{77}H_{144}O_{33}Na]^+$	1620.0	0.1

product. The most dominant series of signals with a maximum in intensity at $m/z = 1585.5$ can be assigned to the sodium molecule ions of the different chain lengths of the desired structure **6**. Two additional series of signals with minor intensity are assigned to the potassium molecule ions of **6** as well as to the sodium molecule ions of the diene functionalized PEG **3**. Even though signals which correspond to structure **3** appear in the spectrum, a careful MS-MS investigation shows that their occurrence can be explained by the appearance of the retro HDA of **6** under the applied ESI-MS conditions (see experimental section) and not by an incomplete conversion of **3**. However, the intensity of signals of **3** in the ESI-MS measurement is relatively low and also depended on the measuring conditions and did therefore vary in intensity between different measurements. For the degradation studies performed in the framework of this study, the ESI-MS conditions were kept constant to prevent such difficulties in signal intensity. As the spectra should be as quantitative as possible, constant ionization conditions for all samples were given priority over mass accuracy, which could have been increased by specific tuning of the spectrometer.

A zoom of the 1582−1626 *m/z* region, which includes the signal with the highest intensity, is shown in Figure 2b. The experimental *m/z* values of the three peaks in this zoom region are compared to the theoretical values of the corresponding ion assignments as summarized in Table 2 confirming the structures of PEG **6** and **3**.

For the confirmation of structure **7** as the reaction product of the HDA cycloaddition between PEG **3** and RAFT agent **5** via NMR and ESI-MS methods, similar results as for compound **6** were found. Figure SI-3 (Supporting Information) shows the ^{1}H NMR spectrum of **7**. Also in this case, the disappearance of the signals of two of the four vinylic protons as well as of the methylene group in the allyl position of the starting material **3** after the HDA reaction suggests a successful conversion of **3**. The ESI-MS measurement of PEG **7** (Figure 3a) shows a series of signals with a maximum in intensity at $m/z = 1438.5$ that can be assigned to the sodium molecule ions of the different chain lengths of the desired structure **7**. Additional series of signals with minor intensity are assigned to potassium molecule ions of **7** as well as to the sodium molecule ions of the diene functionalized PEG **3**.

A zoom of the 1436−1480 *m/z* region which includes the signal with the highest intensity is depicted in Figure 3b. The experimental *m/z* values of the three peaks in this zoom region are compared to the theoretical values of the corresponding ion assignments, as summarized in Table 3, confirming the structures of PEG **7** and **3**.

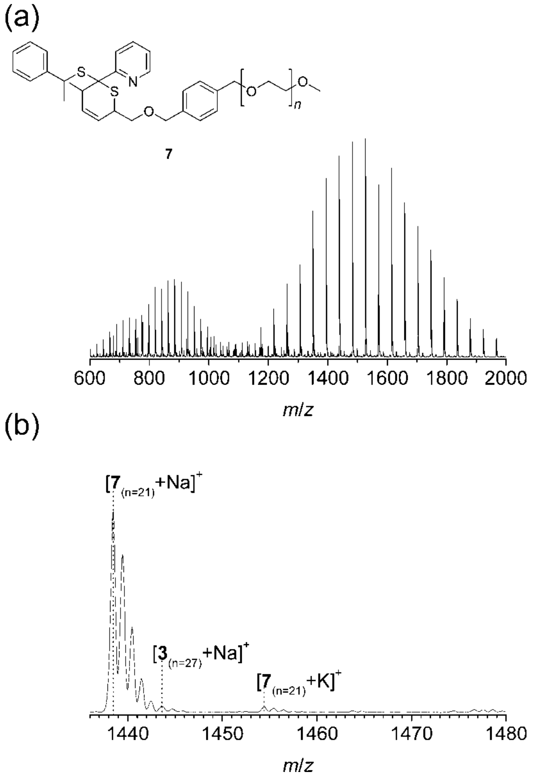

Figure 3. (a) Full ESI-MS spectrum and (b) 1436−1480 *m/z* region of PEG **7** after the HDA cycloaddition between RAFT agent **5** and PEG **3** (trifluoroacetic acid as the catalyst, chloroform, 24 h, 50 °C).

Table 3. Experimental and Theoretical *m/z* Values for the First Peak in the Isotopic Distributions of the Zoom Spectrum in Figure 3b and Their Assignment

m/z_{expt}	ion assignment	formula	m/z_{theor}	$\Delta m/z$
1438.5	PEG $7_{(n=21)}$ + Na$^+$	$[C_{71}H_{117}NO_{23}S_2Na]^+$	1438.7	0.2
1443.6	PEG $3_{(n=27)}$ + Na$^+$	$[C_{69}H_{128}O_{29}Na]^+$	1443.8	0.2
1454.4	PEG $7_{(n=21)}$ + K$^+$	$[C_{71}H_{117}NO_{23}S_2K]^+$	1454.7	0.3

Thermal Stability of PEG 6 and 7. As mentioned in the introduction, it was shown in recent work that poly(styrene) 4-arm star polymers which were prepared via the RAFT HDA approach underwent a complete cleavage of the poly(styrene) arms from the core after being subjected to a high-temperature environment.[13] The actual reaction mechanism which led to the fragmentation, however, was not studied. It is known from thermal stability studies on RAFT agents[4,5] and RAFT polymers[6] that the carbon−sulfur single bonds are the most labile linkage in dithioesters, trithiocarbonates and xanthates. Depending on the stabilizing influence of different R and Z groups, elimination reactions can already occur at a temperature of 120 °C. In the 3,6-dihydro-2*H*-thiopyran ring of compound **6** and **7**, however, the dithioester function is converted into a dithioketal which is expected to increase the thermal stability in terms of elimination reactions because—due to the absence of a thiocarbonyl function—a concerted elimination mechanism is not possible. Another conceivable reaction path of the HDA end-groups in **6** and **7** at elevated temperatures is the retro HDA reaction. In fact, the HDA adduct of methyl (diisopropylphosphoryl)dithioformate and cyclopentadiene which contains a 3,6-dihydro-2*H*-thiopyran ring, similar to that in structure **6** and **7**, was reported to undergo the retro HDA reaction at elevated temperature.[21] In order to investigate this behavior of temperature induced cleavage on the 3,6-dihydro-2*H*-thiopyran functionalized polymers **6** and **7**, these were subjected to different temperature environments (80−180 °C) for 24 h and ESI-MS measurements were performed on the reaction products to study the formed products. Therefore, PEG **6** and **7** were dissolved in toluene and subjected for 24 h to different temperatures ranging from 80 to 180 °C.

Figure 4a shows the ESI-MS spectra of PEG **6** after 24 h at 80, 100, 120 and 160 °C as representative examples. The spectrum after treatment at 80 °C is essentially identical to the original spectrum (Figure 2a). It contains a series of signals, which is assigned to the sodium molecule ions of PEG **6**, as the most dominant species confirming the stability of the 3,6-dihydro-2*H*-thiopyran under these conditions. With increasing temperature, however, it is clearly possible to observe a decrease in relative intensity of the signals of PEG **6** and an increase of

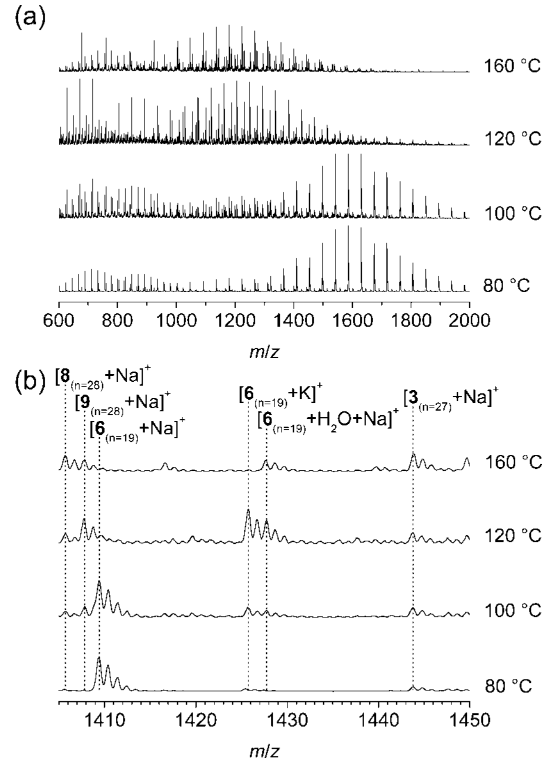

Figure 4. ESI-MS spectra of PEG **6** after treatment at different temperatures (80, 100, 120 and 160 °C) in toluene solution for 24 h; (a) full spectra and (b) 1405−1450 *m/z* region.

Table 4. Experimental and Theoretical *m/z* Values for the First Peak in the Isotopic Distributions of the Zoom Spectrum in Figure 4b and Their Assignment

m/z_{expt}	ion assignment	formula	m/z_{theor}	$\Delta m/z$
1405.7	PEG $8_{(n=28)}$ + Na^+	$[C_{65}H_{122}O_{30}Na]^+$	1405.8	0.1
1407.7	PEG $9_{(n=28)}$ + Na^+	$[C_{65}H_{124}O_{30}Na]^+$	1407.8	0.1
1409.5	PEG $6_{(n=19)}$ + Na^+	$[C_{66}H_{115}O_{24}PS_2Na]^+$	1409.7	0.2
1425.7	PEG $6_{(n=19)}$ + K^+	$[C_{66}H_{115}O_{24}PS_2K]^+$	1425.7	0
1427.6	PEG $6_{(n=19)}$ + H_2O + Na^+	$[C_{66}H_{117}O_{25}PS_2Na]^+$	1427.7	0.1
1443.9	PEG $3_{(n=27)}$ + Na^+	$[C_{69}H_{128}O_{29}Na]^+$	1443.8	0.1

five new series of signals shifted to lower *m/z* values. A shift of the signal distributions to lower masses indicates that their occurrence is a result of fragmentation reactions in which certain end-group fragments are cleaved. A zoom of the 1405−1450 *m/z* region is shown in Figure 4b which covers the best possible overlap of the different distributions. Three of the six peaks in the zoom region are known species and can be assigned as PEG **6** (sodium and potassium molecule ions) and PEG **3** (sodium molecule ions). A comparison with the theoretical values of the corresponding ion assignments is summarized in Table 4. The relative intensity of the signals of PEG **3** increases in the spectra with rising temperature whereas the signal intensity of PEG **6** decreases. This behavior is consistent with the occurrence of the retro HDA reaction which should become more dominant at higher temperatures. In order to assign the three remaining signals, the masses of possible fragment structures were calculated and compared with the obtained *m/z* values. They can be identified as 4-methyl benzaldehyde and 4-methyl benzylalcohol terminated PEG **8** and **9** (Scheme 5), respectively, as well as to a water-adduct of PEG **6** or any structural isomer of those compounds. Table 4 includes a comparison with the theoretical values of the corresponding ion assignments, which were further confirmed with high-resolution Q-TOF measurements. In Q-TOF, the mass of **8** and **9** was confirmed within $\Delta m/z = 0.060$ and $\Delta m/z = 0.001$, respectively, which can be seen as a very satisfactory match between theoretical values and experiment.

Scheme 5. 4-Methyl Benzaldehyde and 4-Methyl Benzylalcohol Terminated PEG 8 and 9, Respectively

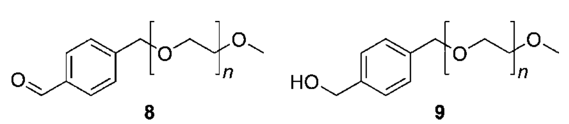

The mechanism which led to the occurrence of structure **8** and **9** is not fully understood. There is some indication that the ether bond in **6** may constitute another weak link in addition to the 3,6-dihydro-2*H*-thiopyran function. In addition, the origin of the water-adduct (which was confirmed by MS-MS measurements to be chemically bonded) could not be resolved yet. However, compounds **3**, **8** and **9**, which are the most dominant signals in the spectrum after treatment at 160 °C, all represent fragmented species of the initial 3,6-dihydro-2*H*-thiopyran end-capped PEG **6** in which the 1-phenylethyl group mimicked a RAFT polymer chain. They therefore confirm the observation of fragmentation of polymer segments in previous reports,[13] even though this fragmentation does not occur in an uniform mechanism.

For the study of the thermal stability of the 2-pyridin-2-yl-3,6-dihydro-2*H*-thiopyran in PEG **7** similar experiments were performed as for PEG **6**. Figure 5a shows the complete ESI-MS spectra of PEG **7** after 24 h at 120, 160 and 180 °C as representative examples. The spectrum after treatment at 120 °C is nearly identical to the original spectrum (Figure 3a) and contains the series of signals, which is assigned to the sodium molecule ions of PEG **7**, as the most dominant species. Due to the preservation of structure **7** after 24 h at 120 °C, no experiments at lower temperature were performed. With increasing temperature, however, a decrease in relative intensity of the signals of PEG **7** and an increase of a series of signals which is shifted to lower *m/z* values is clearly observed. A zoom

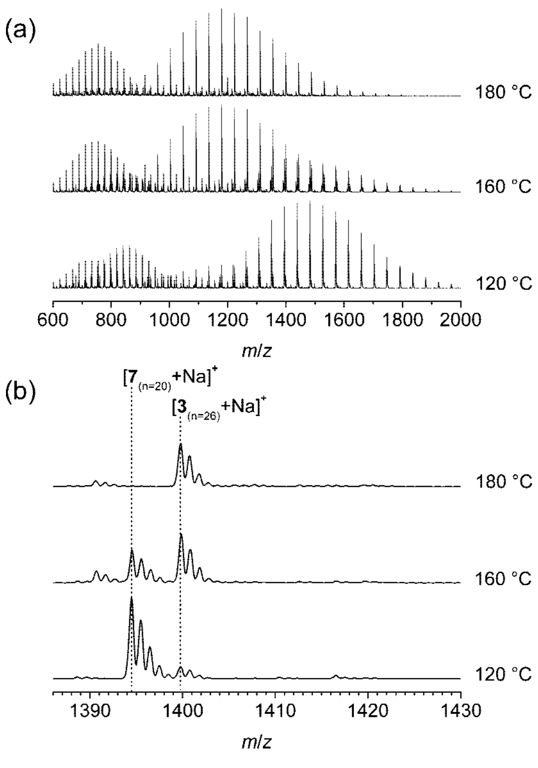

Figure 5. ESI-MS spectra of PEG **7** after treatment at different temperatures (120, 160, and 180 °C) in toluene solution for 24 h: (a) full spectra and (b) 1386−1430 *m/z* region.

Table 5. Experimental and Theoretical *m/z* Values for the First Peak in the Isotopic Distributions of the Zoom Spectrum in Figure 5b and Their Assignment

m/z_{expt}	ion assignment	formula	m/z_{theor}	$\Delta m/z$
1394.5	PEG $7_{(n=20)}$ + Na^+	$[C_{69}H_{113}NO_{22}S_2Na]^+$	1394.7	0.2
1399.9	PEG $3_{(n=26)}$ + Na^+	$[C_{67}H_{124}O_{28}Na]^+$	1399.8	0.1

of the 1286−1430 *m/z* region is shown in Figure 5b again covering the best possible overlap of the two distributions. The experimental *m/z* values of the peaks in this zoom region are compared to the theoretical values of the corresponding ion assignments, as summarized in Table 5.

The relative intensity of the signals of PEG **3** increases, whereby the signal intensity of PEG **7** decreases in the spectra with rising temperature. This behavior is consistent with the occurrence of the retro HDA reaction which should become more dominant with higher temperatures. Interestingly, even after subjecting the PEG **7** to 180 °C for 24 h, the diene functionalized PEG **2** is the only detectable reaction product and no further side reaction is observed as was done with PEG **6**.

In comparison, the stability tests toward thermal conditions showed for the diethoxyphosphoryl derivative **6** the preservation of the polymer end-groups after 24 h at temperatures up to 80 °C. At higher temperatures degradation reactions of the 3,6-dihydro-2*H*-thiopyran ring including the retro HDA reaction occur. A complete fragmentation is observed after 24 h at 160 °C. The pyridinyl derivative **7** is found to be slightly more temperature stable, since its structure is still unaffected at conditions up to 24 h at 120 °C and full cleavage may only be observed after 24 h at 180 °C. In this case the mechanism, which leads to the fragmentation, is the retro HDA reaction and the resulting diene functionalized polymer is the only detected product species. Hence, the polymeric starting material for the HDA reaction is obtained allowing for a full reversibility of the conjugation method. The origin of species **8** and **9** as fragments of PEG **6** remains uncertain for the moment. However, to allow for more detailed insights, the fragmentation counterpart needs to be known. As in the present study a model compound was used, no information on the counterpart could be obtained by ESI-MS.

pH Stability of PEG 6 and 7. Thiocarbonyl compounds are known to be unstable toward hydrolysis. Investigations on thioacylating reagents showed degrees of hydrolysis of dithioesters after 24 h at around 10% (pH = 7.5 − 8.5, 20 °C).[31] It was also shown in investigations on aqueous RAFT polymerizations that this behavior can be critical for the maintenance of the polymerization control, especially at increased pH values.[7] In the present structure in PEG **6** and **7**, the 3,6-dihydro-2*H*-thiopyran, which can be regarded as an acyclic dithioketal, is expected to show a significant higher stability toward hydrolysis. This expectation is based on reports about dithioketals as protection groups of carbonyl functions which show a high resistance against acidic and basic conditions.[32] In order to study the stability of the 3,6-dihydro-2*H*-thiopyran functionalized polymers **6** and **7** in acidic and basic aqueous solution, they have been subjected to different pH environments (pH = 0, 1, 13 and 14) for 24 h at room temperature. The sharp conditions from both sides of the pH range were chosen in order to cover both extremes of acidic and basic environments implying that stability under these harsh conditions would allow for the interpolation over the complete pH range.

Figure 6a shows the ESI-MS spectra of PEG **6** after 24 h of exposure to aqueous media at strong acidic and basic conditions (pH = 0, 1, 13 or 14). The four spectra are essentially identical to the original spectrum (Figure 2a) and contain the series of signals which is assigned to the sodium molecule ions of PEG **6** as the most dominant species. A zoom of the 1627−1671 *m/z* region, which includes the maxima of the distributions, is shown in Figure 6b. The experimental *m/z* values of the peaks in this zoom region are compared to the theoretical values of the corresponding ion assignments, as summarized in Table 6, confirming the structures of PEG **6**.

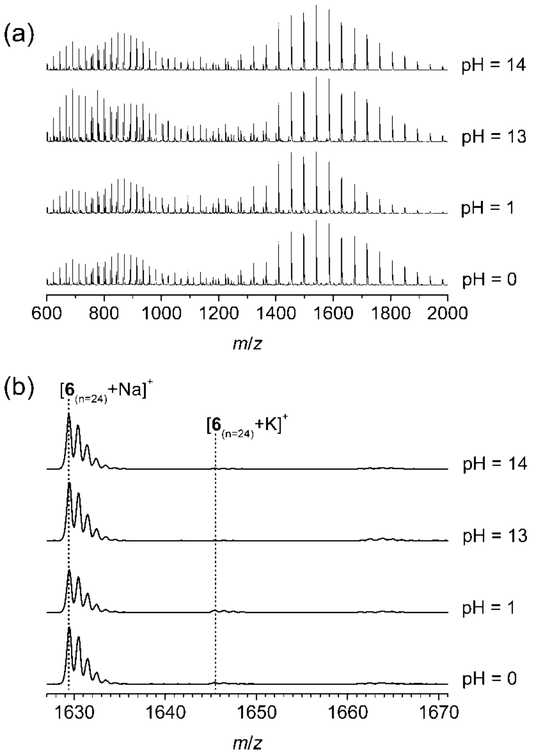

Figure 6. ESI-MS spectra of PEG **6** after exposure to aqueous media at strong acidic and basic conditions (pH = 0, 1, 13 or 14): (a) full spectra; (b) 1627−1671 *m/z* region.

Table 6. Experimental and Theoretical *m/z* Values for the First Peak in the Isotopic Distributions of the Zoom Spectrum in Figure 6b and Their Assignment

m/z_{expt}	ion assignment	formula	m/z_{theor}	$\Delta m/z$
1629.5	PEG $6_{(n=24)}$ + Na^+	$[C_{76}H_{135}O_{29}PS_2Na]^+$	1629.8	0.3
1645.5	PEG $6_{(n=24)}$ + K^+	$[C_{76}H_{135}O_{29}PS_2K]^+$	1645.8	0.3

Similar results were found for the study on the stability toward hydrolysis of the 2-pyridin-2-yl-3,6-dihydro-2*H*-thiopyran in PEG **7**. Figure 7a shows the full ESI-MS spectra of PEG **7** after 24 h in aqueous solution at different pH values (pH = 0, 1, 13 or 14). Also here, all four spectra show the signals of the initial HDA adduct **7** as the most dominant species with no significant byproduct. Signals which can be assigned to PEG **3** are found of minor intensity as seen in the original spectrum of PEG **7** (Figure 3a). Their appearance is most likely due to the retro HDA occurring during electrospray ionization.

A zoom of the 1436−1480 *m/z* region, which includes the maxima of the signal distributions, is shown in Figure 7b. The experimental *m/z* values of the peaks in this zoom region are compared to the theoretical values of the corresponding ion assignments, as summarized in Table 7, confirming the structures of PEG **7** and PEG **3**.

According to the ESI-MS measurements, the 3,6-dihydro-2*H*-thiopyran structure of PEG **6** and **7** show no tendency to hydrolyze under the applied conditions, which confirms the high stability of such dithioketal compounds against basic or acidic aqueous media.

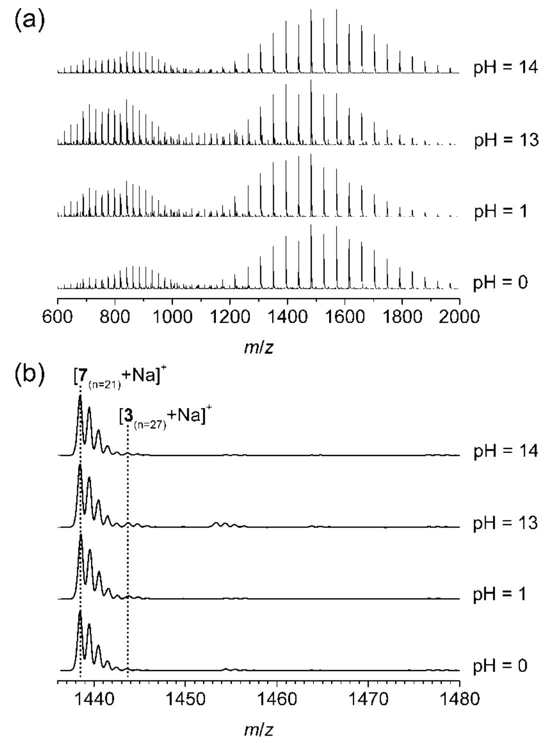

Figure 7. ESI-MS spectra of PEG **7** after exposure to aqueous media at strong acidic and basic conditions (pH = 0, 1, 13 or 14): (a) full spectra; (b) 1436−1480 *m/z* region.

Table 7. Experimental and Theoretical *m/z* Values for the First Peak in the Isotopic Distributions of the Zoom Spectrum in Figure 7b and Their Assignment

m/z_{expt}	ion assignment	formula	m/z_{theor}	$\Delta m/z$
1438.5	PEG $7_{(n=21)}$ + Na^+	$[C_{71}H_{117}NO_{23}S_2Na]^+$	1438.7	0.2
1443.8	PEG $3_{(n=27)}$ + Na^+	$[C_{69}H_{128}O_{29}Na]^+$	1443.8	0

Conclusions

3,6-Dihydro-2*H*-thiopyran functionalized PEG **6** and **7** were obtained after the HDA cycloaddition between a diene functionalized PEG and 1-phenylethyl (diethoxyphosphoryl)dithioformate and 1-phenylethyl pyridin-2-yldithioformate, respectively. The stability of the HDA generated end-groups of these polymers was tested under different thermal and pH conditions whereby ESI-MS was employed to map the generated products. Clearly, the structural stability can be guaranteed at temperatures below 80 and 100 °C for PEG **6** and **7**, respectively. With increasing temperature, however, a fragmentation of the end-group is observed in both cases. Whereas this fragmentation occurs exclusively via the retro HDA in case of **7**, additional side reactions play a role in the end-group fragmentation of **6**. However, in both cases, a complete disappearance of the starting material is observed at temperatures above 160 and 180 °C for PEG **6** and **7**, respectively. By transferring the behavior of temperature induced cleavage of the described model compounds to actual RAFT HDA polymer conjugates, it may open up their application as polymer architectures with predetermined fragmentation patterns in fields like molecular imprinting, smart materials, and biomedical devices. In this context, the pyridinyl derivative such as in compound **7** seems to be a very promising candidate because it allows for the quantitative reversibility of the conjugation method via the retro HDA reaction and hence—at least in principle—for the implementation of conjugation−cleavage cycles. Both derivatives showed an excellent stability toward hydrolysis in aqueous media under strong acidic or strong basic conditions allowing for the utilization of the RAFT HDA approach in aqueous systems over a broad range of conditions.

Acknowledgment. C.V.S. acknowledges financial support from the German Academic Exchange Service (DAAD). Additionally, we thank Dr. L. Barner and I. Jacenyik for the excellent management of CAMD as well as Prof. Dr. M. Guilhaus from the BMSF facility of the UNSW for the opportunity to perform Q-TOF measurements. C.B.-K. acknowledges continued funding from the Karlsruhe Institute of Technology (KIT) within the framework of the German Excellence Initiative. M.H.S. and C.B.-K. acknowledge funding via an ARC Discovery Grant. MHS acknowledges continued support from the University of New South Wales.

Supporting Information Available: Figures showing ^{1}H NMR spectra of **3**, **6**, and **7**. This information is available free of charge via the Internet at http://pubs.acs.org.

References and Notes

(1) (a) Barner, L.; Davis, T. P.; Stenzel, M. H.; Barner-Kowollik, C. *Macromol. Rapid Commun.* **2007**, *28*, 539–559. (b) Hawker, C. J.; Bosman, A. W.; Harth, E. *Chem. Rev.* **2001**, *101*, 3661–3688. (c) Matyjaszewski, K. *Prog. Polym. Sci.* **2005**, *30*, 858–875.
(2) (a) Rizzardo, E.; Moad, G.; Thang, S. H., RAFT Polymerization in Bulk Monomer or in (Organic) Solution. In *Handbook of RAFT Polymerization*, 1st ed.; Barner-Kowollik, C., Ed.; Wiley-VCH: Weinheim, Germany, 2008; pp 189−234. (b) Moad, G.; Rizzardo, E.; Thang, S. H. *Aust. J. Chem.* **2005**, *58*, 379–410. (c) Moad, G.; Rizzardo, E.; Thang, S. H. *Aust. J. Chem.* **2006**, *59*, 669–692. (d) Moad, G.; Rizzardo, E.; Thang, S. H. *Polymer* **2008**, *49*, 1079–1131.
(3) Barner, L.; Perrier, S., Polymers with Well-Defined End Groups via RAFT-Synthesis, Applications and Postmodification. In *Handbook of RAFT Polymerization*, 1st ed.; Barner-Kowollik, C., Ed.; Wiley-VCH: Weinheim, Germany, 2008; pp 455−482.
(4) Liu, Y.; He, J. P.; Xu, J. T.; Fan, D. Q.; Tang, W.; Yang, Y. L. *Macromolecules* **2005**, *38*, 10332–10335.
(5) Legge, T. M.; Slark, A. T.; Perrier, S. *J. Polym. Sci., Part A: Polym. Chem.* **2006**, *44*, 6980–6987.
(6) Chong, B.; Moad, G.; Rizzardo, E.; Skidmore, M.; Thang, S. H. *Aust. J. Chem.* **2006**, *59*, 755–762.
(7) Thomas, D. B.; Convertine, A. J.; Hester, R. D.; Lowe, A. B.; McCormick, C. L. *Macromolecules* **2004**, *37*, 1735–1741.
(8) Llauro, M. F.; Loiseau, J.; Boisson, F.; Delolme, F.; Ladaviere, C.; Claverie, J. *J. Polym. Sci., Part A: Polym. Chem.* **2004**, *42*, 5439–5462.
(9) (a) Qiu, X. P.; Winnik, F. M. *Macromol. Rapid Commun.* **2006**, *27*, 1648–1653. (b) Qiu, X. P.; Winnik, F. M. *Macromolecules* **2007**, *40*, 872–878. (c) Xu, J. T.; He, J. P.; Fan, D. Q.; Wang, X. J.; Yang, Y. L. *Macromolecules* **2006**, *39*, 8616–8624.
(10) (a) Lowe, A. B.; Sumerlin, B. S.; Donovan, M. S.; McCormick, C. L. *J. Am. Chem. Soc.* **2002**, *124*, 11562–11563. (b) Scales, C. W.; Convertine, A. J.; McCormick, C. L. *Biomacromolecules* **2006**, *7*, 1389–1392. (c) Spain, S. G.; Albertin, L.; Cameron, N. R. *Chem. Commun.* **2006**, 4198–4200.
(11) Vana, P.; Albertin, L.; Barner, L.; Davis, T. P.; Barner-Kowollik, C. *J. Polym. Sci., Part A: Polym. Chem.* **2002**, *40*, 4032–4037.
(12) Sinnwell, S.; Inglis, A. J.; Davis, T. P.; Stenzel, M. H.; Barner-Kowollik, C. *Chem. Commun.* **2008**, 2052–2054.
(13) Inglis, A. J.; Sinnwell, S.; Davis, T. P.; Stenzel, M. H.; Barner-Kowollik, C. *Macromolecules* **2008**, *41*, 4120–4126.
(14) Sinnwell, S.; Inglis, A. J.; Stenzel, M. H.; Barner-Kowollik, C. *Macromol. Rapid Commun.* **2008**, *29*, 1090–1096.
(15) Nebhani, L.; Sinnwell, S.; Inglis, A. J.; Stenzel, M. H.; Barner-Kowollik, C.; Barner, L. *Macromol. Rapid Commun.* **2008**, *29*, 1431–1437.
(16) Beslin, P.; Metzner, P. *Tetrahedron Lett.* **1980**, *21*, 4657–4658.
(17) (a) Vyas, D. M.; Hay, G. W. *Can. J. Chem.* **1971**, *49*, 3755–3758. (b) Vyas, D. M.; Hay, G. W. *J. Chem. Soc., Perkin Trans. 1* **1975**, 180–186.
(18) (a) Vedejs, E.; Arnost, M. J.; Dolphin, J. M.; Eustache, J. *J. Org. Chem.* **1980**, *45*, 2601–2604. (b) Kirby, G. W.; Lochead, A. W.; Williamson, S. *J. Chem. Soc., Perkin Trans. 1* **1996**, 977–984.
(19) Portella, C.; Shermolovich, Y. G.; Tschenn, O. *Bull. Soc. Chim. Fr.* **1997**, *134*, 697–702.
(20) (a) Boerma, J. A.; Nilsson, N. H.; Senning, A. *Tetrahedron* **1974**, *30*, 2735–2740. (b) El-Sayed, I.; Ali, O. M.; Fischer, A.; Senning, A. *Heteroat. Chem.* **2003**, *14*, 170–174.
(21) Heuze, B.; Gasparova, R.; Heras, M.; Masson, S. *Tetrahedron Lett.* **2000**, *41*, 7327–7331.

(22) (a) Heras, M.; Gulea, M.; Masson, S. *Chem. Commun.* **2001**, 611–612. (b) Heras, M.; Gulea, M.; Masson, S.; Philouze, C. *Eur. J. Org. Chem.* **2004**, 160–172.

(23) Bastin, R.; Albadri, H.; Gaumont, A. C.; Gulea, M. *Org. Lett.* **2006**, *8*, 1033–1036.

(24) (a) Gondi, S. R.; Vogt, A. P.; Sumerlin, B. S. *Macromolecules* **2007**, *40*, 474–481. (b) Quemener, D.; Davis, T. P.; Barner-Kowollik, C.; Stenzel, M. H. *Chem. Commun.* **2006**, 5051–5053. (c) Ranjan, R.; Brittain, W. J. *Macromol. Rapid Commun.* **2007**, *28*, 2084–2089.

(25) (a) Buback, M.; Frauendorf, H.; Gunzler, F.; Vana, P. *Polymer* **2007**, *48*, 5590–5598. (b) Buback, M.; Frauendorf, H.; Gunzler, F.; Vana, P. *J. Polym. Sci., Part A: Polym. Chem.* **2007**, *45*, 2453–2467. (c) Szablan, Z.; Junkers, T.; Koo, S. P. S.; Lovestead, T. M.; Davis, T. P.; Stenzel, M. H.; Barner-Kowollik, C. *Macromolecules* **2007**, *40*, 6820–6833. (d) Chaffey-Millar, H.; Hart-Smith, G.; Barner-Kowollik, C. *J. Polym. Sci., Part A: Polym. Chem.* **2008**, *46*, 1873–1892. (e) Gruendling, T.; Hart-Smith, G.; Davis, T. P.; Stenzel, M. H.; Barner-Kowollik, C. *Macromolecules* **2008**, *41*, 1966–1971. (f) Barner-Kowollik, C.; Davis, T. P.; Stenzel, M. H. *Polymer* **2004**, *45*, 7791–7805.

(26) Bennet, F.; Lovestead, T. M.; Barker, P. J.; Davis, T. P.; Stenzel, M. H.; Barner-Kowollik, C. *Macromol. Rapid Commun.* **2007**, *28*, 1593–1600.

(27) (a) Junkers, T.; Bennet, F.; Koo, S. P. S.; Barner-Kowollik, C. *J. Polym. Sci., Part A: Polym. Chem.* **2008**, *46*, 3433–3437. (b) Feldermann, A.; Ah Toy, A.; Davis, T. P.; Stenzel, M. H.; Bamer-Kowollik, C. *Polymer* **2005**, *46*, 8448–8457.

(28) Abrunhosa, I.; Gulea, M.; Masson, S. *Synthesis* **2004**, 928–934.

(29) Laus, M.; Papa, R.; Sparnacci, K.; Alberti, A.; Benaglia, M.; Macciantelli, D. *Macromolecules* **2001**, *34*, 7269–7275.

(30) Alberti, A.; Benaglia, M.; Guerra, M.; Gulea, M.; Hapiot, P.; Laus, M.; Macciantelli, D.; Masson, S.; Postma, A.; Sparnacci, K. *Macromolecules* **2005**, *38*, 7610–7618.

(31) Levesque, G.; Arsene, P.; Fanneau-Bellenger, V.; Pham, T. N. *Biomacromolecules* **2000**, *1*, 400–406.

(32) Wuts, P. G. M.; Greene, T. W., In *Protective Groups in Organic Synthesis*, 4th ed.; Wuts, P. G. M., Ed. Wiley-Interscience: Hoboken, NJ, 2006; pp 477−500.

MA8013959